15th IFK
Proc. of the 15th International Fluid Power Conference <Symposium/Conference>
<DOI>

Design and Application of a Prediction Model of the Loads and Mission Profile for Hydraulic Steering System in Heavy-Duty Off-Road Vehicles

M. Bertoli, B. Zardin, M. Borghi

Enzo Ferrari Department of Engineering, University of Modena and Reggio Emilia, Modena, Italy 41125
matteo.bertoli@unimore.it, barbara.zardin@unimore.it, massimo.borghi@unimore.it.

Abstract.

Centralized hydraulic circuits are typically employed to actuate the steering system and other different users in off-road vehicles, particularly in agricultural tractors. These solutions, while robust and widely adopted, lead to high energy demands and significant contributions to overall fuel consumption and greenhouse gas emissions. This study forms part of a wider academic research project aimed at developing an experimental platform integrated with virtual models to study alternative architectures, with the objective of improving energy efficiency and sustainability of heavy-duty off-road vehicles. In particular, this work is dedicated to developing a mathematical model that predicts the loads acting on the hydraulic steering actuator during working cycles. Indeed, measuring the loads acting on a tractor's steering system during real-world operation is challenging and costly. Field tests require the vehicle to be equipped with sensors and to undergo controlled work cycles on different terrains, which demand considerable time, resources and logistical complexity. Predictive models thus offer a clear advantage, addressing the lack of experimental data by generating virtual but realistic steering loads. The novel contribution of this paper is a simulation framework that, accounting for the vehicle's front axle load, soil type, and tire sinkage, creates realistic duty cycles to feed a hardware-in-the-loop test bench. These parameters, in fact, critically affect the forces transmitted to the hydraulic actuator. The model is based on a detailed kinematic study of the front axle with core terramechanics concepts to define the tire–soil interaction. The mathematical model was corroborated by comparing the results with those of a multibody simulation model of the front axle. The virtual assembly includes the main rigid bodies and a double-rod hydraulic steering cylinder. This simulation shows the mechanical behavior under both static and dynamic loads, providing force estimates across different realistic operating scenarios. We derived the modeling assumptions and boundary conditions from relevant literature on heavy-duty vehicle dynamics. As a future application, the results obtained from this validated model will be employed to actuate the solenoid valves of a load generating system in a test bench, thereby exerting the desired working conditions on the hydraulic power steering system.

Keywords. Hydraulic, steering, heavy duty vehicles, test rig, multibody simulation

1. INTRODUCTION

Hydraulic steering systems in heavy-duty off-road vehicles are typically driven by centralized load sensing circuits. While robust and widely adopted, these architectures result in high energy demands and significant hydraulic losses. Recent studies highlight the impact of these systems on fuel consumption and greenhouse gas emissions, especially during multi-actuator operations where overload pressure and compensator-induced dissipation are prevalent [1, 2]. Driven by growing industrial interest in sustainability and energy efficiency in the agricultural sector, research focuses on alternative hydraulic layouts. These include independent metering valve systems, electronically controlled variable displacement pumps and electro-hydraulic power steering systems with solenoid valves [3, 4, 5, 6]. Such configurations improve control flexibility and decrease power losses, particularly when integrated with digital control strategies that interact with mechanical models [7, 8].

However, the performance evaluation of hydraulic steering systems in realistic operating conditions is still a complicated and resource-intensive process. Field testing requires advanced instrumentation, controlled cycles on different terrains and considerable logistical effort [9, 10, 11]. In this context, predictive modeling proves to be an effective method for estimating steering loads, thereby avoiding the necessity for extensive experimental testing. Prior research validated the effectiveness of multibody simulations and terramechanics-based models for tire–soil interactions [12, 13, 14, 15, 16]. Angelucci et al. [17] explore the applicability of terra-mechanical models to optimize soil-tire interaction and highlight a gain on performance. Analytical foundations for predictive models are based on multidisciplinary contributions: Hegendus introduces dimensional analysis and plate penetration techniques to derive soil parameters [18], while Bekker's model estimates ground deformation, sinking and shear stresses induced by vehicular loads [19]. Thus, Taborek provided the theory for studying kinematic behavior on vehicle steering mechanics, while Terzaghi's theoretical soil mechanics further clarified the role of cohesion, internal friction, and effective stress in soil failure [20, 21]. These cross-disciplinary notions are used in several engineering fields, e.g. robotics: Jia et al. [22] and Ishigami et al. [23] built a predictive model for a rover focused on tire-soil interaction, which can be integrated into multibody simulations. Instead, Patel et al. [24] applied Hegendus terramechanics to shovel-ground interaction in excavators. In conclusion, Cao et al. [25] pointed out the importance of axle friction and alignment forces, during pivot steering alongside terra-mechanical contributions. Despite the extensive literature on terramechanics and vehicle dynamics, a significant research gap remains in the availability of reliable, experimental-like load data for the validation of steering systems without relying on costly field campaigns. Drawing inspiration from rover studies, this research adapts the methodology to the agricultural sector. The novelty lies in the integration of these analytical foundations into a comprehensive multibody co-simulation approach. The result is a 'virtual sensor' capable of generating reliable duty cycles for hardware-in-the-loop validation.

2. EXPERIMENTAL TEST BENCH LAYOUT

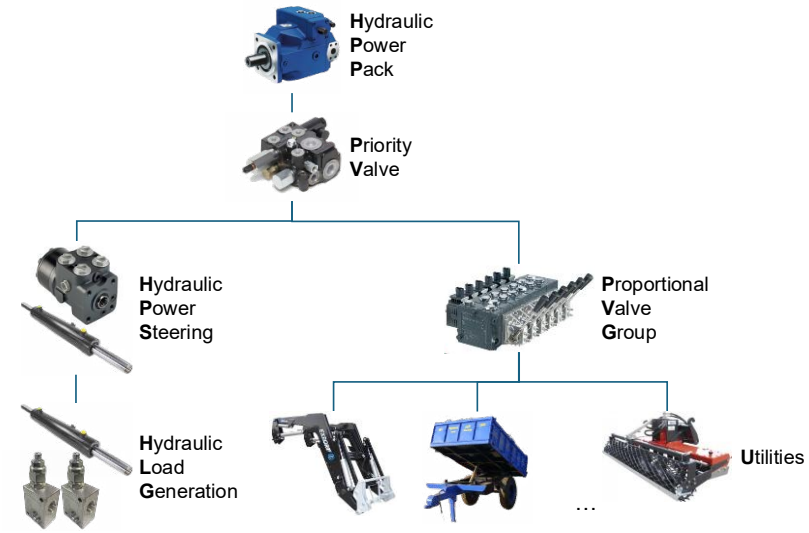

Figure 2.1. Baseline configuration layout

The design of an experimental bench for testing hydraulic and electro-hydraulic components, typically used in heavy duty vehicles, needs a method to replicate a duty cycle on the primary user, i.e. the steering system. Therefore, the primary purpose of the platform is to exert on the hydraulic power steering (HPS) system the same forces and displacements that would be observed during actual field operation. Although the platform does not include a physical front axle, this apparent hardware limitation is in fact advantageous: the platform core is a digital twin that replicates the front axle and its kinematics through the hydraulic load generation (HLG) system. Different axle geometries, kinematics or tractor dimensions can be simulated by updating the model, without mechanical reconfiguration.

The layout also includes secondary users, such as lifting actuators and orbital motors, or in general users that can be mounted on a tractor. Hydraulic power distribution is managed by a priority valve. The described layout is known as the baseline configuration and is illustrated in Figure 2.1. Obviously, the platform's modular design allows for the configuration of alternative hydraulic architectures. For example, it can operate without a priority valve and with users powered independently. Nevertheless, the focus of this work is the steering function. Therefore, alternative circuit configurations and secondary users, including the priority valve, are not considered in this context. The analysis addresses HPS and HLG subsystems.

2.1. HPS Main Components

Figure 2.2 illustrates the hydraulic layout of the steering branch of the experimental platform. HPS replicates the steering architecture typically utilized in utility tractor. We chose two representative components:

- Danfoss OSPC80LS steering unit (4 in Fig. 2.2) [26]

- Ognibene 57/35 × 190 mm double acting steering cylinder with through rod (3A) [27]

The OSPC80LS is connected to the steering wheel and adjusts the flow to the cylinder based on the pilot's manual input. The cylinder is selected with a through rod, similar to many of those installed on front axles.

2.2. HLG Main Components

The innovative core of the test bench is the HLG system. This unit provides an autonomous short-circuited load system, unlike conventional rigs, which include safety valves to release oil in case of unexpected pressure spikes. This represents an effective solution for avoiding power saturation of the bench control unit. The main components of the HLG are:

- Ognibene 57/35 × 190 mm double-acting steering cylinder with through rod (3B) [27]
- Hydraforce TS12-27 two-way proportional solenoid valves (5A and 5B) [28]
- Anti-cavitation and anti-shock safety valves (6)

Note that we chose the same actuator as the steering one, as it provides the same area ratios on both sides. However, the platform is not limited to this configuration. In fact, if different cylinders are used, a correction factor derived from the chamber area ratio could be considered. The proportional pressure relief valves operate alternately depending on the steering direction. Their opening is controlled by a PWM signal generated by the data acquisition and control system (DAQ). However, a key consideration for this configuration is the need for high-frequency acquisition to quickly control valve opening, thus ensuring stability within the simulated duty cycle.

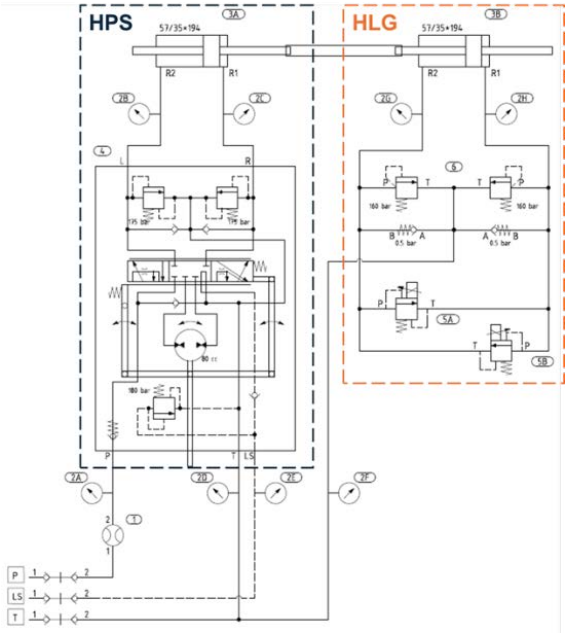

Figure 2.2. Hydraulic circuit of power steering (HPS) and load generation (HLG) systems

2.3. DAQ Design

The platform's data acquisition and control system is implemented on a National Instruments CompactRIO (cRIO), a real-time embedded controller integrating a real-time processor, an FPGA, and modular I/O. Acquisition is handled by the NI Scan Engine, which performs a deterministic I/O scan cycle over a user-defined scan period (typically 1 ms, up to ~1 kHz), ensuring synchronous sampling of multiple signals, such as hydraulic pressures, flow rates, angular steering position, linear displacement, and load cell measurements. Scan Engine logic is easier to program because you can access I/O variables directly in LabVIEW Real-Time as shared variables, but the maximum cycle speed is limited by the scan speed. PWM signals for Hydraforce T12-27 are also generated through the Scan Engine. High-frequency FPGA acquisition is not required in this context.

Based on this hardware setup, three operating scenarios are supported. The first uses fixed pressure thresholds on proportional valves, simplifying the identification of steady-state behavior. This mode is used for preliminary hardware calibration and does not rely on the simulation model. The second scenario uses a look-up table that correlates predefined steering resistances with wheel angular positions. The validated model presented in this paper is specifically aimed at generating the data for this second scenario. The last scenario, representing the next step of the research work, provides continuous co-simulation during the experimental test. In this setup, the DAQ integrates real-time simulation outputs to dynamically adjust the valve opening, effectively connecting the physical steering system with the digital twin.

3. ANALYTIC APPROACH

This chapter presents the analytical approach used to validate the virtual model of the front steering axle and to estimate the soil-induced resistance on the vehicle. Modeling is broken down into two problems: the kinematics and dynamics of the steering axle, which provides how steering inputs turn into wheel motion and reaction forces; and the terra-mechanical model, which estimates ground-tire forces in relation to terrain characteristics and tire/load conditions. The aims of the analytical formulation are to obtain a reduced-order dynamic system of the front axle and to define a mathematical model that correlates the lateral forces on the tire surface to the steering cylinder based on the steering angle.

3.1. Assumptions and Reference Frames

The steering axle and components are modeled as rigid bodies, the vehicle is considered stationary, and friction in the kinematics is assumed negligible due to lack of literature data. Furthermore, a limiting scenario is considered in which the minimal imprint that the tire can create in the soil corresponds to the square of its thickness.

We considered both a fixed O_{xyz} and a rotating $O_{x'y'z'}$ reference system. The O_{xyz} frame is located along the cylindrical joint connecting the hub and the axle, and it is aligned perpendicularly to the ground plane. The mobile reference system $O_{x'y'z'}$ is obtained from the former by a γ-rotation around the z-axis, which is the steering angle, and a δ-rotation around the x-axis, which is the kingpin angle. Naming O the fixed frame O_{xyz} and O' the rotating frame $O_{x'y'z'}$, Equation 3.1 provides the rotation matrix to pass from O to O'.

$$R_{O\to O'} = R_z(\gamma)R_x(\delta) = \begin{bmatrix} \cos\gamma & -\sin\gamma\cos\delta & \sin\gamma\sin\delta \\ \sin\gamma & \cos\gamma\cos\delta & -\cos\gamma\sin\delta \\ 0 & \sin\delta & \cos\delta \end{bmatrix} \quad (3.1)$$

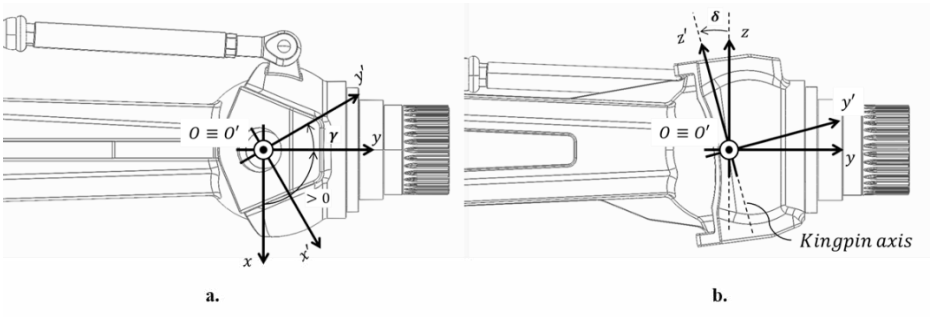

Figure 3.1. Fixed reference frame O_{xyz} and mobile $O_{x'y'z'}$ on xy-plane (a) and yz-plane (b)

3.2. Front Axle Analysis: Kinematics and Dynamics

The steering axle is approximated as a crank mechanism with deflected thrust, as Figure 3.2 depicts. For the sake of clarity, we use the same reference systems as common methods. Note that α, named the crank angle, can be written as $\alpha(\gamma)$ if $\widehat{AOG} = \pi/2$, where G is the tire center of gravity. Furthermore, the domain of $\alpha \notin [0; 2\pi]$ but is limited due to the kinematics of the axis. Eq. 3.2 represents the OAB vector closing triangle in terms of its coordinates.

$$A = \begin{Bmatrix} a\cos\alpha \\ a\sin\alpha \end{Bmatrix} \quad B = \begin{Bmatrix} s \\ h \end{Bmatrix} \quad (3.2)$$

where h is a fixed dimension that depends on the axle geometries, s is the cylinder stroke. Using Eq. 3.3 we obtain the length of the rod AB.

$$b = \sqrt{(s - a\cos\alpha)^2 + (h - a\sin\alpha)^2} \quad (3.3)$$

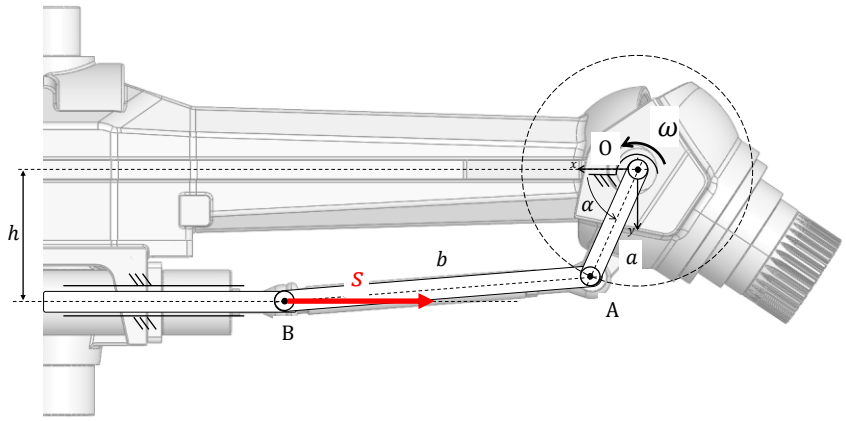

Figure 3.2. Kinematics right steered analysis

This condition results in a quadratic equation in s from which the solution, described in Eq. 3.4, is obtained.

$$s(\alpha) = a\cos\alpha + \sqrt{b^2 - (h - a\sin\alpha)^2} \tag{3.4}$$

It is now possible to derive Eq. 3.4 to obtain the speed of the steering actuator. Similarly, acceleration can be obtained by deriving the velocity.

Subsequently, we focus on dynamic analysis, with the system being modeled again as a crank mechanism with deflected thrust. The aim of this formulation is to guarantee that M_{res}, denoting the torque at hub, is balanced from the cylinder force. We present the right steering scenario, illustrated in Figure 3.3a.

However, this approach can also be applied to left steering. Therefore, the rod angle β can be expressed in Eq. 3.5.

$$\beta(\alpha) = \cos^{-1}\left(\frac{h - a\sin\alpha}{b}\right) \tag{3.5}$$

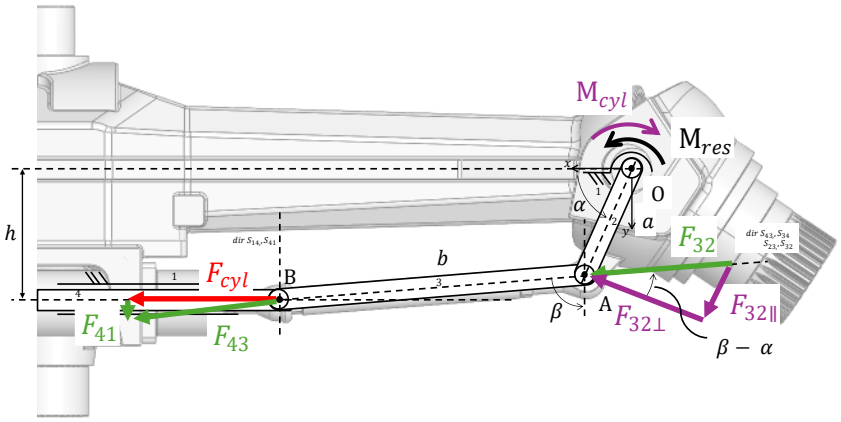

a.

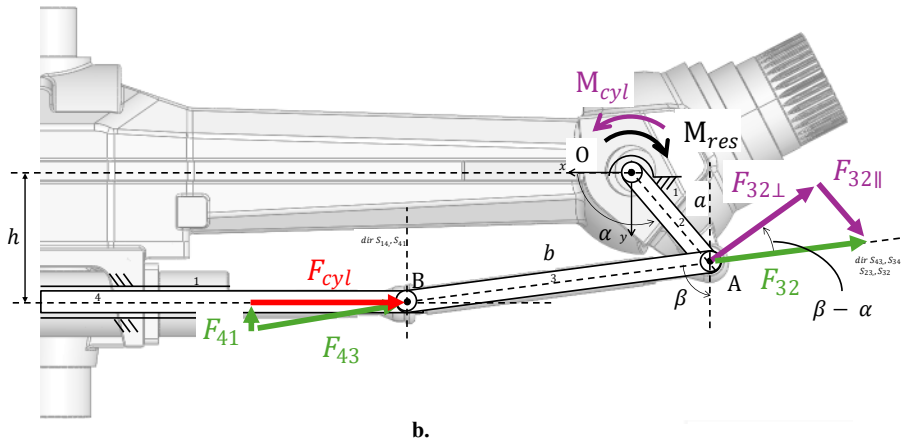

b.

Figure 3.3. Dynamic right (a) and left (b) steered analysis

F_{cyl} represents the force applied by the cylinder in the direction of the guide. The axial force acting on the connecting rod AB is obtained by projecting it along the slider's axis, while the perpendicular component to the crank AO produces the resisting torque at the hub M_{res} around point O. Equation 3.6 illustrates the computation of M_{res}.

$$M_{res} = aF_{32,\perp} = aF_{32}\cos(\beta - \alpha) = a\frac{F_{cyl}}{\sin\beta}\cos(\beta - \alpha) \tag{3.6}$$

In conclusion, M_{res} is moved from the fixed frame to the mobile frame $O_{x'y'z'}$ by means of the rotation matrix $R_{O\to O'}$, to represent the hub torque on kingpin axis. Note that this model refers to a specific axle configuration and, in the future, with a library of axles available, the same method can be applied to other configurations.

3.3. Kingpin Torque Calculation and Terramechanics Analysis

In this subchapter, the resistance torque acting on the steering hub is estimated by combining different theoretical frameworks from kingpin analysis to terramechanics-based tire–soil interaction models. We chose a customized analytical approach rather than commercial "black-box" models in order to ensure flexibility and explicit control over critical variables, particularly tire sinkage (h). This allows for rapid reconfiguration of soil-vehicle parameters and direct definition of sinking levels, which are the main determinants of lateral loads on the steering. The current approach assumes a stationary vehicle and a pivot steering; therefore, future developments will extend the model to include vehicle motion, allowing the simulation of dynamic efforts.

3.3.1. Normal Contact Pressure and Sinkage

According to Bekker's pressure–sinkage relationship, the normal contact pressure $\sigma(h)$ between tire and soil is expressed as Eq. 3.7.

$$\sigma(h) = \left(\frac{k_c}{b} + k_\varphi\right)h^n \tag{3.7}$$

where k_c, k_φ, n are soil parameters, h is sinkage, and b is the tire width. The wheel sinkage $h(\theta)$ at arbitrary angular position θ is given geometrically by Eq. 3.8.

$$h(\theta) = r\,(\cos\theta - \cos\theta_s) \tag{3.8}$$

The contact angle θ_s is derived from the vertical load balance,

$$W = \int_{-\theta_s}^{\theta_s} \sigma(\theta)\, br\, \cos\theta\, d\theta \tag{3.9}$$

as W is the known tractor load on the wheel. The static sinkage is then evaluated using the geometric relation described in Eq. 3.10.

$$h_s = r(1 - \cos\theta_s) \tag{3.10}$$

where r is the tire radius and θ_s is the contact angle. Finally, the local pressure distribution can be represented as a function of θ, as shown in Eq. 3.11.

$$\sigma(\theta) = \left(\frac{k_c}{b} + k_\varphi\right)[r\,(\cos\theta - \cos\theta_s)]^n \tag{3.11}$$

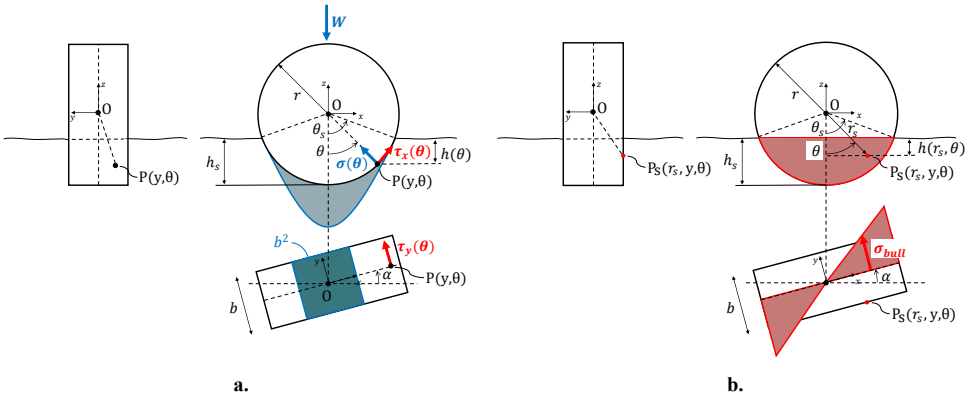

Figure 3.4. Representation of the contributions of normal pressure in $P(y,\theta)$ (a) and bulldozing in $P_s(r_s,y,\theta)$ (b) on the wheel

3.3.2. Shear Stress

The maximum shear stress that can be transferred between the ground and the tire is limited by the weakest contact, determined by the tire-to-ground friction and the internal cut resistance of the ground (Mohr-Coulomb). This relation is described in Eq. 3.12.

$$\tau_{max} = min\ (\mu_s\sigma, c + \sigma \tan\phi) \tag{3.12}$$

where μ_s is the sliding friction coefficient, c is the soil cohesion, and φ is the soil internal friction angle. For the integration of this contribution, we consider the point $P(y,\theta)$ as

$$P(y,\theta) = [r\ \sin\theta \quad y \quad -r\cos\theta]^T \tag{3.13}$$

In the stationary vehicle assumption ($v_x = 0$), slip ratio and slip angle lose physical meaning, so the Janosi–Hanamoto formulation is excluded. It will be introduced in future model extensions to account for longitudinal motion.

3.3.3. Bulldozing Resistance

In addition to shear stress, the soil exerts resistance on the lateral sinkage tire surface. We consider the point $P_s(r_s,y,\theta)$ as Figure 3.4 (a) depicts.

$$P_s(r_s,\ y,\theta) = [r_s\ \sin\theta \quad y \quad -r_s\cos\theta]^T \tag{3.14}$$

Thus, the relative sinkage is evaluated using Eq. 3.15.

$$h(r_s,\theta) = r_s\ \cos\theta - r\ \cos\theta_s \tag{3.15}$$

Following Hegedus model, the stress per unit width is evaluated using Eq. 3.16.

$$\sigma_{bull}(r_s,y,\theta) = D_1\left[c\ h(r_s,\theta) + D_2\frac{\rho_d h(r_s,\theta)^2}{2}\right] \tag{3.16}$$

In the equation above D_1 and D_2 represent geometric coefficients derived from the soil internal friction angle, while ρ_d is the soil density.

3.3.4. Steering Aligning Torque

Due to kingpin inclination, steering must overcome soil resistance and generates a restoring torque. The steering aligning torque is evaluated using Eq. 3.17.

$$M_\theta = -W[e + (r - h_s)\tan\delta]\sin(2\delta)\sin\left(\frac{\gamma}{2}\right) \tag{3.17}$$

where e is the kingpin offset and δ the kingpin angle. This torque tends to realign the wheel toward the neutral position.

3.3.5. Resulting Force and Moments

Lateral (Y-direction) friction forces are computed by integrating over the cylindrical surface element $rd\theta dy$, which characterizes the interface between the wheel and soil (Figure 3.5).

$$F_y = \int_{-b/2}^{b/2}\int_{-\theta_s}^{\theta_s}\left(r\cdot\tau_y(\theta)\right)dyd\theta \tag{3.18}$$

An additional contribution from soil bulldozing must be considered, integrated over the lateral surface increment $r_s\ d\theta dr_s$ within the sink region of the tire.

$$F_{bull} = \int_{r-h(\theta)}^{r}\int_{-\theta_s}^{\theta_s}\sigma_{bull}(\theta)dr_s d\theta \tag{3.19}$$

The corresponding resisting torque is then evaluated using Eq. 3.20.

$$M_{res} = M_z = \int r\ sin\theta\ dF_y + \int r_s\ sin\theta\ dF_{bull} + M_\theta \tag{3.20}$$

In conclusion, M_{res} is moved from the fixed frame to the mobile frame $O_{x'y'z'}$ by means of the rotation matrix $R_{O\to O'}$ (Eq. 3.1).

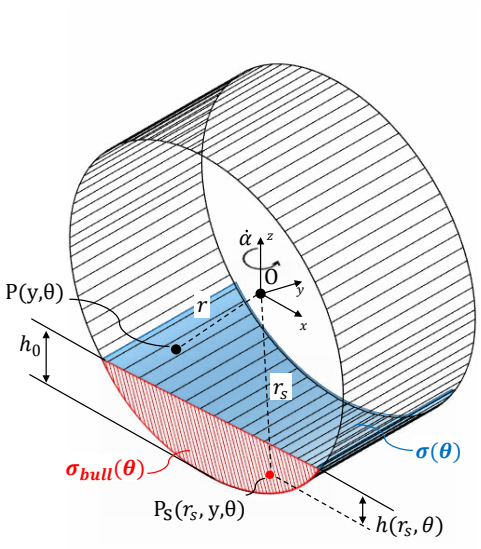

Figure 3.5. Integrals graphical representation of sigma and shear stresses on a tire

4. MULTIBODY APPROACH

The analytical formulation is then translated into a virtual prototype developed in a multi-body environment. In the present work, the modeling strategy is divided into two parts: the development of the steering axle model in ADAMS [29] and the implementation of the control logic in Simulink [30], which together forms the basis for co-simulating the complete steering system.

4.1. Front Axle Analysis: ADAMS model

The steering geometry was first designed in CAD and then imported into ADAMS for the definition of kinematic constraints and dynamic interactions. Some rigid components were merged according to their relative motion to maintain computational efficiency. For instance, the steering knuckle and hub were combined into one unit, while the cylinder of the hydraulic tie-rod assembly was incorporated into the housing.

Kinematic constraints were implemented to replicate the physical linkages, such as revolute joints at the kingpins, translation motion for the actuator rods, and spherical joints at the ball connections between the hubs and brackets.

The model dynamic behavior is introduced by applying a torque on the hubs joint aligned with the kingpin axis. This resistant torque, calculated in Simulink according to the selected operating scenario (for example clay soil with the New Holland T4.75 vehicle without cabin), reproduces the terra-mechanical resistance on the steering system. At the same time, the force exerted by the hydraulic actuator along its sliding axis is measured as the fundamental output of the multi-body model.

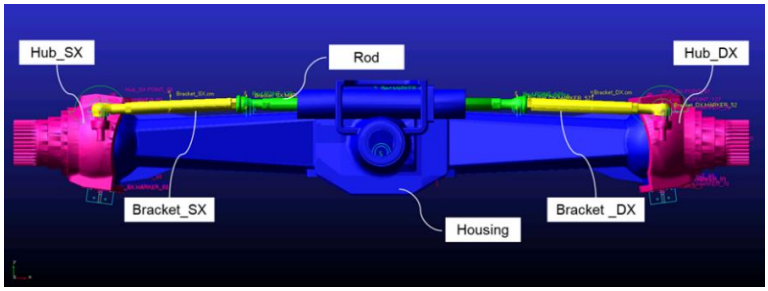

Figure 4.1. CAD model imported to ADAMS and creating constraints

4.2. Simulink Control Loop

The control subsystem was implemented in MATLAB/Simulink to drive the multibody model developed in ADAMS. The Simulink model is structured around different functional blocks, which together reproduce the dynamics of the steering bench and the input control to the hydraulic actuator.

The key parameters for the selected vehicle–ground configuration are read from .csv files, based on the user choices provided through the drop-down menu selections (1 in Fig. 4.2). In Tables 4.1 and 4.2, we provide parameters that characterize respectively soils and tractors, which relate to the results of the simulations discussed in the following chapter. It is important to note that we have assumed a vehicle weight distribution of 45% front and 55% rear. Also, the vehicle was evaluated without ballast and tools.

The control input of the system is the steering wheel angular position. Currently, a lock-to-lock maneuver is simulated; however, this signal will be logged in real-time concerning the angular position of the platform's steering wheel (2). These data and the geometric properties of the bench components are used to derive the displacement of the steering cylinder.

Blocks (3) and (4) contain MATLAB functions for computing the wheel hub-resistant torque $M(\gamma, k_{tractor}, k_{soil})$ and the actuator position $s(\theta_w, V_c)$, derived from the analytical model described in the previous sections.

The interface between Simulink and ADAMS was created using Adams Control/Plants (5), which exports the multibody model to a block that can be directly used in Simulink. Furthermore, a closed-loop is implemented to dynamically use the actual steering angle in the terramechanics function (3).

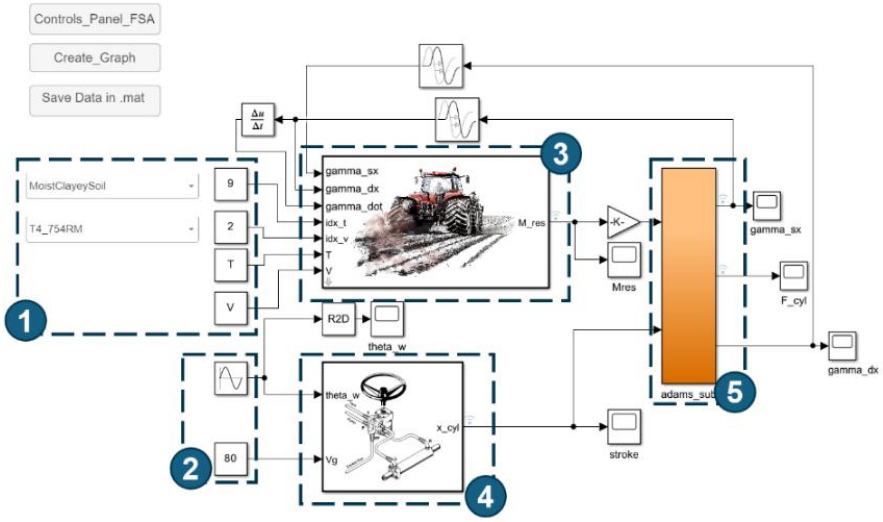

Figure 4.2. Simulink model with block for co-simulation with ADAMS

Table 4.1
Parameters for soil characterization [20] [21] [31].

Terrain Name	μ	Moist	ρ_d	n	k_c	k_φ	c	ϕ
Unit.		%	$\frac{kN}{m^3}$		$\frac{kN}{m^{n+1}}$	$\frac{kN}{m^{n+2}}$	Pa	deg
Asphalt (A)	0.75	0	0	0	0	0	0	0
Standard Sandy Loam (SSL)	0.45	15	16	0.7	5.27	1515.04	1720	29
Fertile Loam (FL)	0.45	24	14	1.01	0.06	5880	3100	29.8
Moist Heavy Clay (MHC)	0.3	55	20	0.11	1.87	103.27	20690	6

Table 4.2
Parameters for vehicle characterization [32] [33].

Tractor Name	Weight on front	b	r	e	δ
Unit.	N	mm	mm	mm	deg
T4.75.4RM	8829	280	450	225	7.5
T6.180	27755	480	670	225	7.5

4.3. Co-simulation Setup

To realize the interfacing between the multibody model in ADAMS and the control model in Simulink, the ADAMS/Controls plugin is used. This tool allows the export of the ADAMS model as a block "plant", i.e. a template that defines the co-simulation inputs and outputs, into Simulink model. This block is a dynamic system that receives commands and returns kinematic/dynamic measurements to the control loop. From Simulink to ADAMS, the following state variables are provided:

- Torque corrections derived from the feedback law, M_{res}.
- Actuator rod displacement, s.

From ADAMS to Simulink, the following state variables are provided:

- Actual steering angle of the hubs, γ.
- Actuator force, F_{cyl}.

ADAMS simulates one time step while maintaining the received inputs constant. Then, Simulink simulates for the step, keeping the ADAMS outputs constant. The new values are then exchanged, and this loop continues.

5. RESULTS

The first set of results, shown in Figure 5.1 (a–b), presents a comparison between the analytical formulation and the multibody simulation. A lock-to-lock maneuver was simulated that corresponded to four complete turns of the steering wheel. In this manner, the steering actuator executes its complete stroke within the bench configuration.

Note that, due to the modeled mechanism, the full stroke of the actuator corresponds to a steering sweep of approximately 60° on the hub. Therefore, the steering angle asymmetry shown in Figure 5.1b is inherent to the steering axle kinematics. Future developments may include testing different CAD configurations. Finally Figure 5.1 (c–d) illustrates the steering cylinder force and the resisting hub torque, respectively, throughout the simulated duty cycle. The clear overlap between the curves indicates a strong correlation between the analytical and multibody models, with negligible deviations, confirming the accuracy of the kinematic and dynamic implementation of the virtual model.

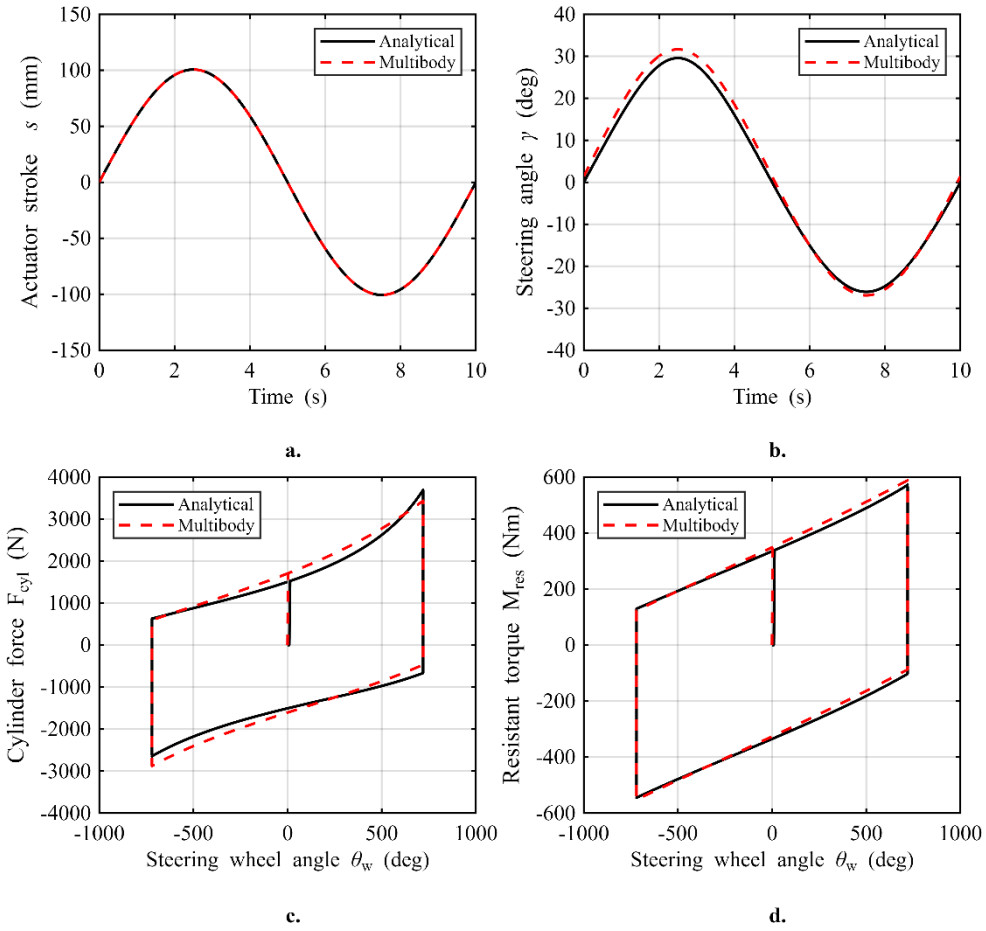

Figure 5.1. Simulation results for T4.75.4RM on Fertile Loam

Figure 5.2 illustrates a comparative analysis between the lighter New Holland T4.75 and the heavier T6.180 across four simulated soil conditions: Asphalt (A), Standard Sandy Loam (SSL), Fertile Loam (FL), and Moist Heavy Clay (MHC). For the New Holland T4.75.4RM (Figure 5.2 a-b), the impact of soil type on steering loads is minimal: the resulting resistance torques is similar in different scenarios. In fact, with a low vertical load, the deformation of the contact area and the corresponding soil shear stress are minimal, thereby reducing the variability of the steering resistance.

In contrast, in the case of the heavier vehicle (Figure 5.2 c-d), the influence of soil characteristics becomes significant. The heavier load on the front axle increases the tire-soil contact pressure, resulting in greater static sinkage (approximately 10 cm). As a result, more cohesive or compact soils generate the strongest torques, while softer soils allow easier lateral movement of tires. A distinct behavior can be observed on clayey soil (MHC): this soil provides low surface resistance, which is at most balanced by the self-aligning torque due to the kingpin's geometry during the rod's return movement. It is important to highlight that this kind of soil provided the greatest resistance when the tire sinkage is severe (for instance, during overload or "stuck" scenarios).

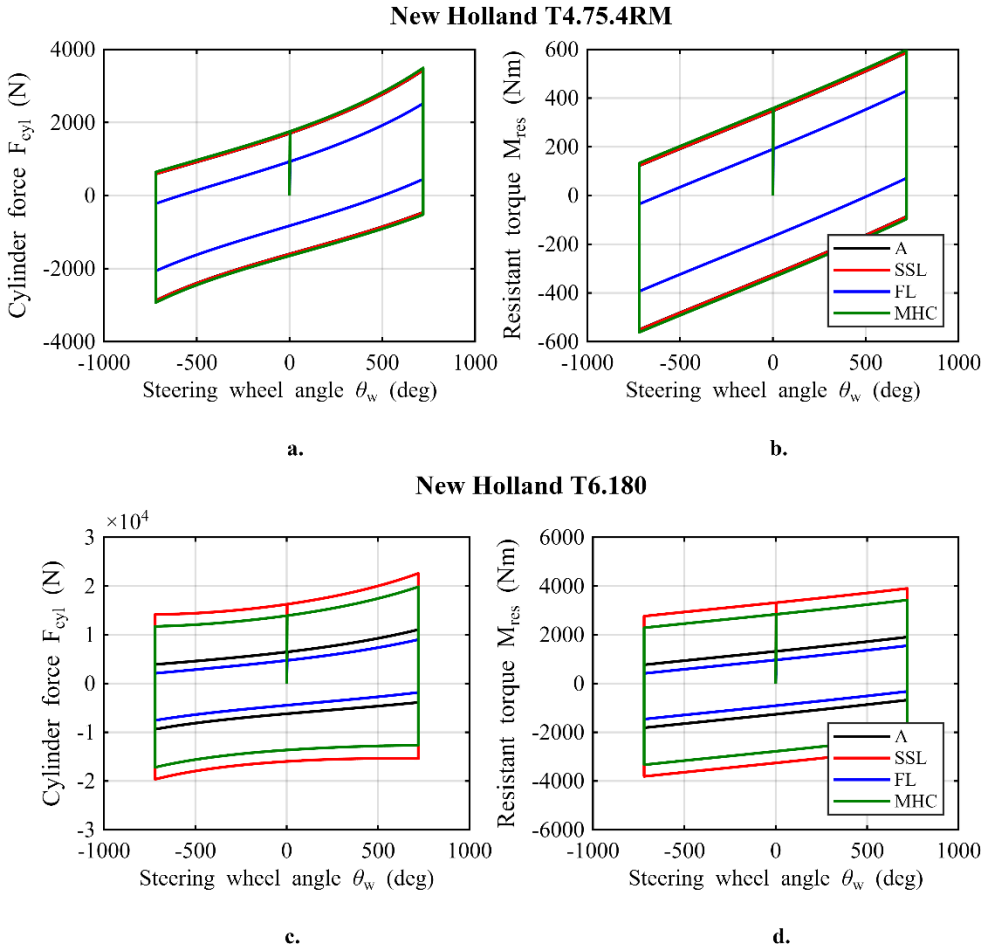

Figure 5.2. Comparison of the simulation results for New Holland T4.75.4RM (a-b) and New Holland T6.180 (c-d) on different soil

6. CONCLUSIONS

This work supports the performance evaluation of hydraulic steering systems in heavy vehicles, highlighting the role of digitalization in laboratory reproduction of operational scenarios through a digital twin approach. The proposed layout represents modular and scalable architecture, facilitating the acquisition of hydraulic and mechanical data that are often estimated during vehicle tests. This model represents the preliminary step of a forward-looking Hardware-in-the-Loop (HIL) approach. Despite the simplifying hypotheses adopted, the results appear robust and physically consistent, supported by the tuning of the terra-mechanical parameters according to the analytic approach.

Driven by growing industrial interest in improving the efficiency of on-board hydraulic systems, especially steering, future research will aim to simulate different front axle configurations. In addition, future developments will extend the model to include vehicle dynamics, influence of tire inflation pressure and non-stationary steering maneuvers.

Finally, the implementation of a Digital Twin, characterized by real-time bidirectional data exchange and synchronization between the digital model and the physical platform, represents the goal of this research project. Future works will focus on this final integration step and on the experimental validation of the complete co-simulation loop. This approach lays the groundwork for future advancements in virtual testing methodologies, contributing to more sustainable and efficient development of off-road vehicle systems.

ACKNOWLEDGMENTS

The authors would like to acknowledge CNH Industrial for the collaboration in the modeling and research activity. The authors would also like to thank Walvoil SpA and Ognibene SpA for providing their support in terms of know–how and materials. This research has been funded by PR-FESR EMILIA ROMAGNA 2021-2027 in the context of the project FACT Future of Agricultural Tractors (ID 38034, CUP E37G22000510007).

7. REFERENCES

[1] M. Borghi, B. Zardin, F. Pintore, F. Belluzzi, 'Energy Saving in the Hydraulic Circuit of Agricultural Tractor', Energy Procedia 45, 2014, https://doi.org/10.1016/j.egypro.2014.01.038.

[2] D. Padovani, P. Dimitriou, T. Minav, 'Challenges and solutions for designing Energy-Efficient and Low-Pollutant Machines in Off-Road hydraulics', Energy Conversion and Management, 2024, https://doi.org/10.1016/j.ecmx.2024.100526.

[3] A. Gaiola, B. Zardin, P. Casoli, et. al., 'The Hydraulic Power Generation and Transmission on Agricultural Tractors: feasible architectures to reduce dissipation and fuel consumption – Part 1', E3S Web of Conferences 197, 2020, https://doi.org/10.1051/e3sconf/202019707009.

[4] P. Casoli, B. Zardin, et. al., 'The Hydraulic Power Generation and Transmission on Agricultural Tractors: feasible architectures to reduce dissipation and fuel consumption – Part 2', E3S Web of Conferences 197, 2020, https://doi.org/10.1051/e3sconf/202019707010.

[5] H. Du, et. al., 'The design, simulation, and experiment of high-accuracy multi-axle electro-hydraulic control servo steering system', Advances in Mechanical Engineering, 2016, https://doi.org/10.1177/1687814016674383.

[6] B. Zardin, M. Borghi, F. Gherardini, N. Zanasi, 'Modelling and Simulation of a Hydrostatic Steering System for Agricultural Tractors', Energies, 2018, https://doi.org/10.3390/en11010230.

[7] Y. Gültekin, et. al., 'Modelling and Simulation of Power Steering System for Agricultural Tractors', International Journal of Advances on Automotive and Technology, 2016.

[8] G. Panetta, F. Mancarella, M. Borghi, et. al., 'Dynamic Modelling of an Off-Road Vehicle for the Design of a Semiactive, Hydropneumatic Spring-Damper System', ASME International Mechanical Engineering Congress and Exposition Proceedings, 2015.

[9] I. Schröder, T. Schmidt, J. Krusborg, C. Woernle, 'Parametrization of a Real-Time Vehicle Model from Driving Tests for HiL Testing of Hydraulic Steering Systems', New Trends in Mechanism and Machine Science, EuCoMeS, 2020.

[10] J.A. Pytka, et. at., 'An instrumented vehicle for offroad dynamics testing', Journal of Terramechanics 48, 2011, https://doi.org/10.1016/j.jterra.2011.06.003.

[11] L. Angelucci, M. Mattetti, ‘The development of reference working cycles for agricultural tractors’, Biosystems Engineering, 2024, https://doi.org/10.1016/j.biosystemseng.2024.04.004.
[12] M. Martelli, S. Gessi, P. Marani, et. al., ‘Comprehensive lumped parameter and multibody approach for the dynamic simulation of agricultural tractors with tyre–soil interaction’, IET Cyber-Systems and Robotics, 2023, https://doi.org/10.1049/csy2.12092.
[13] F. Mocera, A. Somà, A. Nicolini, ‘Grousers Effect in Tracked Vehicle Multibody Dynamics with Deformable Terrain Contact Model’, Appl. Sci., 2020, https://doi.org/10.3390/app10186581.
[14] J. Rekem, et. al.,‘Multi-Body Model of Agricultural Tractor for Vibration Transmission Investigation’, Appl. Sci., 2024, https://doi.org/10.3390/app14188451.
[15] H. Yarmohamadi, V. Berbyuk, ‘Kinematic and dynamic analysis of a heavy truck with individual front suspension’, Vehicle System Dynamics, 2013.
[16] S. Laughery et. al., ‘Off-Road Vehicle Locomotion Using Bekker's Model’, SPIE, Orlando, 2000.
[17] L. Angelucci, M. Varani, F. Pinet, et. al., ‘The role of tyres and soil conditions in enhancing the efficiency of agricultural tractors’, Soil and Tillage Research, 2025.
[18] E. Hegedus, ‘A simplified method for the determination of bulldozing resistance’, Land Locomotion Research, Laboratory, Army Tank Automotive Command Report, 61, 1960.
[19] M.G. Bekker, ‘Introduction to Terrain-Vehicle Systems’, University of Michigan Press, Ann Arbor, MI, 1969.
[20] J. J. Taborek, ‘Mechanics of Vehicles’, Penton Publishing Co., Cleveland, 1957.
[21] K. Terzaghi, ‘Theoretical Soil Mechanics’, John Wiley and Son Inc, USA, 1943.
[22] Z. Jia, et. al., ‘Terramechanics-based wheel–terrain interaction model and its applications to off-road wheeled mobile robots’, Robotica, 30(3), 2012, https://doi.org/10.1017/S0263574711000798.
[23] G. Ishigami, et. al., Terramechanics-Based Model for Steering Maneuver of Planetary Exploration Rovers on Loose Soil, Journal of Field Robotics, 2007, https://doi.org/10.1002/rob.20187.
[24] B. P. Patel and J. M. Prajapati, ‘Evaluation of Resistive Force using Principle of Soil Mechanics for Mini Hydraulic Backhoe Excavator’, International Journal of Machine Learning and Computing, Vol. 2, No. 4, 2012.
[25] D. Cao, et. al., ‘Study on Low-Speed Steering Resistance Torque of Vehicles Considering Friction between Tire and Pavement’, Appl. Sci., 2019, https://doi.org/10.3390/app9051015.
[26] Danfoss, Hydraulic Power Steering Systems Catalogue, Danfoss Power Solutions.
[27] Ognibene Power, Hydraulic Steering Cylinders Catalogue, Ognibene S.p.A.
[28] HydraForce, TS12-27 Solenoid Valve Technical Catalogue, HydraForce Inc.
[29] MSC Software Corporation, Adams 2023: Multibody Dynamics Simulation Software.
[30] MathWorks Inc., Simulink: Dynamic System Simulation for MATLAB, Release R2024b.
[31] J.Y. Wong, ‘Theory of Ground Vehicles’, 3rd ed., New York, Wiley, 1997.
[32] New Holland Agriculture, T4 Series Tractor Technical Datasheet, CNH Industrial.
[33] New Holland Agriculture, T6 Series Tractor Technical Datasheet, CNH Industrial.

Biographies

Matteo Bertoli obtained a bachelor's degree in mechanical engineering from University of Ferrara in 2021 and master's degree in mechanical engineering at the "Enzo Ferrari" Engineering Department, University of Modena and Reggio Emilia, in 2024. After one year as a research fellow, he decided to pursue a PhD, driven by growing interest in fluid power applications and hydraulic systems.

Barbara Zardin is an Associate Professor of Fluid Machines and Energy Systems. Her research focuses especially on evaluating and improving the efficiency of fluid power systems and components for mobile applications. She has written over 40 research papers and articles, and is currently the local principal investigator for the University of Modena and Reggio Emilia on the European project H2REF-DEMO (co-funded by the European Union's "Horizon. Europe" programme under the "Clean Hydrogen Partnership", grant agreement no. 101101517), and the PR-FESR Emilia-Romagna 2021–2027 project, "FACT: Future of Agricultural Tractors" (ID 38034, CUP E37G22000510007).

Massimo Borghi is a full professor of Fluid Machines and Energy Systems. His research interests span internal combustion engines and fluid power systems and components, including hydrogen applications. He has written over 90 research articles and papers, making significant contributions to the analysis, modelling and simulation of hydraulic pumps, motors and systems for mobile applications (in both the automotive and off-highway sectors).